

Collisionally-excited emission Lines

Excitation and emission in a 2-level atom



Emission Lines

Emission lines result from photon-emitting downward transitions, and provide key information on the emitting objects, e.g. a nebula.

If we measure the photon flux and know the distance to the nebula, we can calculate the total number of radiative transitions.

The total power emitted is given by:

$$E_{21} = hf \int_V N_2 A_{21} dV$$

And the intensity (Wm^{-2}) received at the Earth (for isotropic emission) is :

$$I_\lambda = E_{21} / 4\pi d^2$$

To convert this to a more useful quantity, such as the total number of ions, which would let us infer ionic abundances or ionization levels, we need to know the population in the upper level and the fraction of transitions that are radiative.

These quantities depend on temperatures, densities and atomic physics.

Emission Line Formation

Other factors can also be important:

Do all the photons escape, or are the lines optically thick?

Does interstellar extinction reduce the measured intensity? etc.

Recall that the equation of radiative transfer gives:

$$I = I_0 e^{-\tau} + S(1 - e^{-\tau})$$

Optically Thin case : $\tau \ll 1$, and $e^{-\tau} \approx 1 - \tau$ so that $I = I_0 + \tau(S - I_0)$

If $I_0 > S$, the emergent intensity is less than I_0 , and we see absorption. The amount of absorption is proportional to the optical depth, and hence to the opacity κ_ν .

If $S > I_0$ we see emission. As $S_\nu = \epsilon_\nu / \kappa_\nu$ and $d\tau_\nu = \kappa_\nu ds$, the line shape depends on the emission coefficient ϵ_ν .

If temperature decreases outwards, we see absorption lines, but if it increases, we see emission lines (e.g. in the solar chromosphere where the temperature is significantly higher than in the photosphere)

Emission and Absorption in a two-level atom

2-level atom: level 1 is the ground state and level 2 the first excited state

Einstein coefficients:

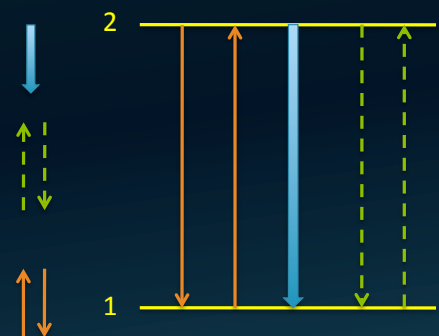
A_{21} spontaneous radiative decay (s^{-1})

B_{12} induced excitation (via photons) [$B_{12} U_\nu s^{-1}$]

B_{21} induced emission (via photons) [$B_{21} U_\nu s^{-1}$]

C_{12} Collisional excitation (via electrons) [$C_{12} N_e s^{-1}$]

C_{21} Collisional de-excitation (via electrons) [$C_{21} N_e s^{-1}$]



Statistical equilibrium: $dN_2/dt = dN_1/dt = 0$

Where N_2 and N_1 are the number densities in the excited and ground states, N_e is the electron density and U_ν is the radiation density:

$$N_2 (C_{21} N_e + B_{21} U_\nu + A_{21}) = N_1 (C_{12} N_e + B_{12} U_\nu)$$

The Two Level Atom

$$N_2 (C_{21} N_e + B_{21} U_v + A_{21}) = N_1 (C_{12} N_e + B_{12} U_v)$$

In regions where the radiation field is weak, the stimulated terms (the B terms) are unimportant, and we can state that

$$B_{21} U_v \ll C_{21} N_e + A_{21} \quad \text{and} \quad B_{12} U_v \ll C_{12} N_e$$

In this case the equation of statistical equilibrium reduces to:

$$N_2/N_1 = C_{12} N_e / (C_{21} N_e + A_{21})$$

Permitted transitions in the UV and optical have spontaneous emission coefficients $A_{21} \geq 10^8 \text{ s}^{-1}$ while the collisional de-excitation coefficients $C_{21} \leq 10^{-12} \text{ m}^3 \text{ s}^{-1}$. If the density is not too high (e.g. in the upper chromosphere and corona in the sun where $N_e \leq 10^{18} \text{ m}^{-3}$, $C_{21} N_e \ll A_{21}$) we can make *the coronal approximation*:

$$N_2/N_1 = C_{12} N_e / A_{21}$$

Thermal distributions

In the coronal approximation, the dominant processes are collisional excitation and spontaneous emission. This does not give detailed balance as $C_{12} N_e$ and A_{21} are not thermodynamically inverse processes. Note that in this case, N_2/N_1 is not given by the Boltzmann distribution.

If the collisional excitation and de-excitation terms (the C terms) are unimportant,

$$N_2/N_1 = B_{12} U_v / (B_{21} U_v + A_{21})$$

If U_v represents a blackbody radiation field, then N_2/N_1 is given by the Boltzmann distribution:

$$\frac{N_2}{N_1} = \frac{g_2}{g_1} e^{-\chi_i / kT}$$

where g_i is the statistical weight of the level, and χ_i is the energy difference between levels 1 and 2. (recall the derivation of the Einstein A and B coefficients)

Thermal distributions

If the radiation field is unimportant and collisional excitation and de-excitation dominates so that

$C_{21} N_e \gg A_{21}$ then

$$N_2/N_1 = C_{12} / C_{21}$$

C_{12} and C_{21} are thermodynamically inverse so detailed balance occurs and N_2/N_1 is again given by the Boltzmann distribution, or

$$\frac{N_2}{N_1} = \frac{C_{12}}{C_{21}} = \frac{g_2}{g_1} e^{-\chi_{12}/kT}$$

In order to apply these expressions in practice, we need information on the physical conditions prevailing in the region of measurement, the electron density N_e and the radiation field U_ν

Collisional excitation and de-excitation rates

We have :

$$C_{21} = C_{12} \frac{g_1}{g_2} e^{\chi_{12}/kT}$$

In statistical equilibrium, the number of excitations = the number of de-excitations, so for a distribution of electrons:

$$N_2 Q_{21}(E') f(v') v' dv' = N_1 Q_{12}(E) f(v) v dv$$

Where Q is the cross section for the collision, v' and v are the electron speeds pre- and post collision and

$$E = 1/2mv^2, E' = 1/2mv'^2, E' - E = E_1 - E_2$$

Where $E_1 - E_2 = \Delta E$ is the energy of the transition = χ_{12}

Collisional cross sections

In thermodynamic equilibrium, the speed distribution $f(v)$ is given by the Maxwellian distribution:

$$4\pi \left(\frac{m}{2\pi kT_e} \right)^{3/2} v^2 \exp(-mv^2 / 2kT_e)$$

And the relationship between the de-excitation and excitation cross sections is then:

$$\frac{Q_{21}(E')}{Q_{12}(E)} = \frac{N_1 v^2 v dv \exp(-mv^2 / 2kT_e)}{N_2 v'^2 v' dv' \exp(-mv'^2 / 2kT_e)}$$

$$\frac{Q_{21}(E')}{Q_{12}(E)} = \frac{N_1}{N_2} \frac{E}{E'} \frac{dE}{dE'} e^{-\chi_{12} / kT_e}$$

But in thermodynamic equilibrium, there is detailed balance and therefore

$$\frac{N_1}{N_2} = \frac{g_1}{g_2} e^{\chi_{12} / kT}$$

$$\Rightarrow \frac{Q_{21}(E')}{Q_{12}(E)} = \frac{g_1}{g_2} \frac{E}{E'}$$

Collisional cross sections

Q is normally expressed in terms of a dimensionless collision strength Ω which is defined to be the same for excitation and de-excitation. i.e.

$$\Omega_{21} = g_2 E' Q_{21} / \pi a_0^2$$

$$\Omega_{12} = g_1 E Q_{12} / \pi a_0^2$$

Where a_0 is the radius of the first Bohr orbit and $\Omega_{21} = \Omega_{12}$.

The collisional de-excitation rate coefficient C_{21} is given by the integral of the cross section, v' and the electron speed distribution. i.e.

$$C_{21} = \int_0^{\infty} v' f(v') Q_{21}(E') dv'$$

Substituting the Maxwellian speed distribution for $f(v')$ and using an average Ω over the energy range gives:

$$C_{21} = 8.6 \times 10^{-12} \frac{\bar{\Omega}_{12}}{g_2} T_e^{-1/2} \quad (m^3 s^{-1})$$

Collisional Coefficients

The collisional excitation rate coefficient C_{12} is given by the integral of the cross section, ν' and the electron speed distribution, but the integral over speed has a threshold value because a minimum energy, corresponding to χ_{12} is required for the excitation to occur:

$$C_{12} = \int_{\nu(\chi_{12})}^{\infty} \nu f(\nu) Q_{12}(E) d\nu$$

Then:

$$C_{12} = 8.6 \times 10^{-12} \frac{\bar{\Omega}_{12}}{g_1} T_e^{-1/2} e^{-\chi_{12}/kT_e}$$

And therefore

$$C_{21} = C_{12} \frac{g_1}{g_2} e^{\chi_{12}/kT_e}$$

gives the relationship between the collisional excitation and de-excitation coefficients. This is important for calculating line intensities and ratios as we will see.

Emission Lines

An emission line results from spontaneous transitions from level 2 to level 1
The number of photons emitted per unit volume, per sec is $A_{21}N_2$ and the line emissivity $j = hc/\lambda A_{21}N_2$

The energy emitted is

$$E_{21} = \frac{hc}{\lambda_{21}} \int_V N_2 A_{21} dV$$

Where V is the volume of the emitting material

In the coronal approximation, this becomes

$$E_{21} = \frac{hc}{\lambda_{21}} \int_V N_1 C_{12} N_e dV$$

So that for most UV and X-ray lines, the emitted flux depends on the collision rate rather than the spontaneous emission coefficient (A value)

The Critical Density

For particular transitions, the applicability of different analyses depends on whether the emitting material has an electron density above or below the critical density.

The critical density is defined as the density at which the collisional de-excitation rate equals the spontaneous decay rate, i.e. $A_{21} = C_{21} N_e$.

Where $N_e \ll N_{crit}$ collisional de-excitation is unimportant : Coronal approximation

Where $N_e \gg N_{crit}$ the level populations are set by the C terms.

Ground-state forbidden transitions in the infrared have A values $< 0.01 \text{ s}^{-1}$ and critical densities in the region of 10^5 to 10^7 cm^{-3} . The energy differences between levels 2 and 1 are small, and so they are insensitive to the electron temperature for $T > 5000\text{K}$

Consider an atom with a split ground state and a large energy interval to the next available level. This is a good approximation to a two-level atom, and is found in the neutral halogens e.g. F I and Cl I and ions in their isoelectronic sequence: e.g. Ne II and Ar II.

There are 5 electrons in the p shell (e.g. Ne II has the configuration $1s^2 2s^2 2p^5$) giving $J = 3/2$ and $1/2$. Neon is an abundant element with I.P. = 21.6 eV, and has a bright line at $12.8\mu\text{m}$ in HII regions

Energy levels

Cl I

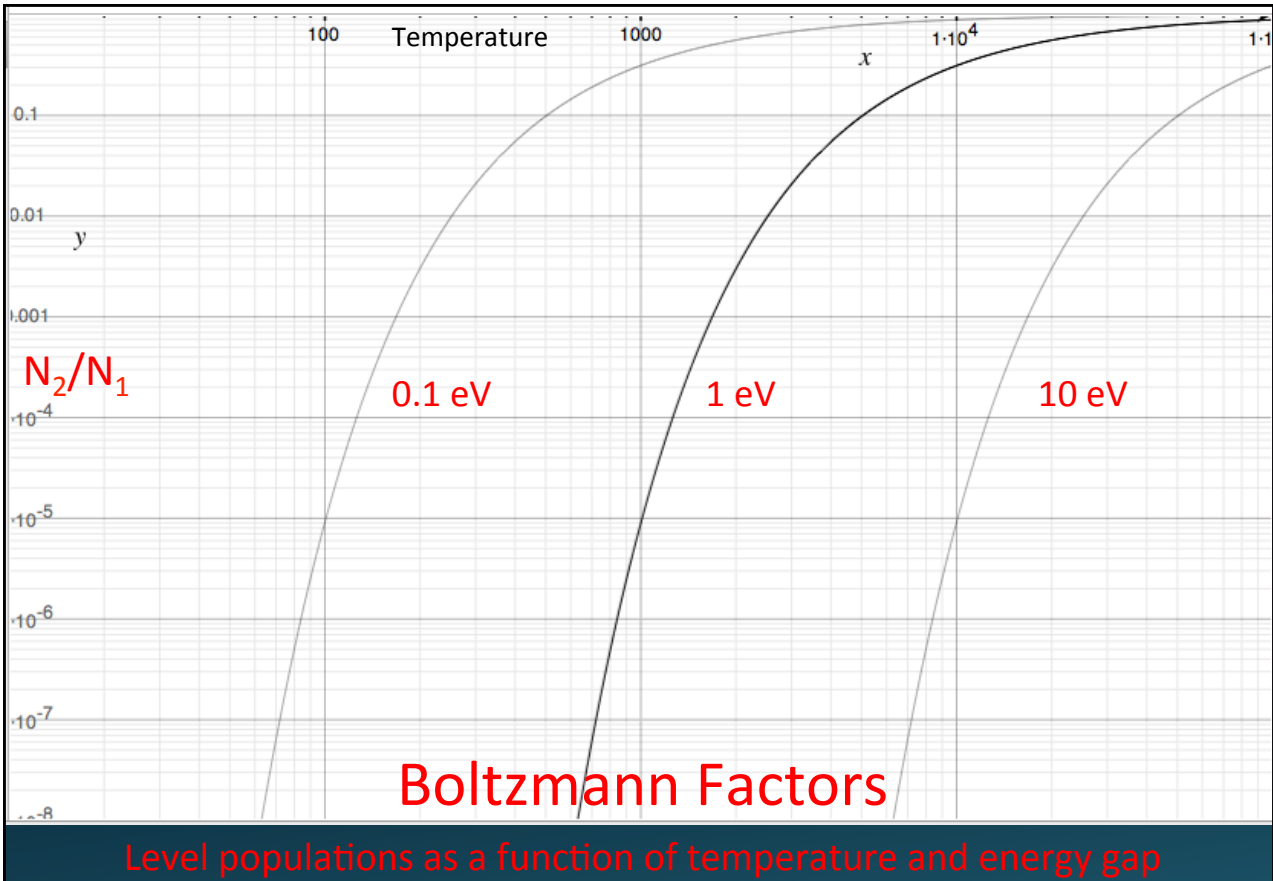
Configuration	Term	J	Level (cm ⁻¹)
$3s^2 3p^5$	$2P^\circ$	$3/2$	0
		$1/2$	882.3515
$3s^2 3p^4(^3P)4s$	4P	$5/2$	71 958.363
		$3/2$	72 488.568
		$1/2$	72 827.038
$3s^2 3p^4(^3P)4s$	2P	$3/2$	74 225.846
		$1/2$	74 865.667
$3s^2 3p^4(^3P)4p$	4P ^o	$5/2$	82 918.893
		$3/2$	83 130.900
		$1/2$	83 364.927

Ne II

Configuration	Term	J	Level (cm ⁻¹)
$2s^2 2p^5$	$2P^\circ$	$3/2$	0.0000
		$1/2$	780.4240
$2s^2 2p^6$	$2S$	$1/2$	217 047.598
$2s^2 2p^4(^3P)3s$	4P	$5/2$	219 130.7609
		$3/2$	219 648.4248
		$1/2$	219 947.4453
$2s^2 2p^4(^3P)3s$	2P	$3/2$	224 087.0092
		$1/2$	224 699.2716
$2s^2 2p^4(^3P)3p$	4P ^o	$5/2$	246 192.4130
		$3/2$	246 415.0144
		$1/2$	246 597.6805

Note that ΔE for the ground state fine structure levels = 882 and 780 cm⁻¹ respectively for Cl I and Ne II. These correspond to 0.11 and 0.10 eV or wavelengths of 11.33 and 12.81 μm . The next levels are at energies factors of 80 and 280 times higher.

From the NIST database <http://physics.nist.gov/PhysRefData/ASD/index.html>



Estimates from ground state IR fine structure lines

For these ground state IR lines, the level populations are insensitive to temperature unless the temperature is too low to populate the upper fine structure level or so high that the excited states are significantly populated - essentially $\Delta E \ll kT_e$ and so the exponential term tends to unity.

With $N_e > N_{crit}$, we have

$$E_{21} = \frac{hc}{\lambda_{21}} \int_V N_2 A_{21} dV$$

The observed line intensity, I_λ from an emitting region = $E/4\pi d^2$ where d is the distance from Earth

and for a uniform density

$$I_\lambda = \frac{E_{21}}{4\pi d^2} = \frac{hc A_{21} N_2 V}{4\pi d^2 \lambda_{21}}$$

Rearranging this in terms of the mass of ions in the upper fine structure level:

$$M_2 = m_a N_2 V = 4\pi d^2 I_\lambda m_a \frac{\lambda_{21}}{hc A_{21}}$$

Where m_a is the mass of the atom and I_λ is the detected line intensity (in $W m^{-2}$). The fraction in the upper level may be given by the Boltzmann distribution.

Supernova 1987A

Exploded in the Large Magellanic Cloud in February 1987.
Distance well determined at 50kpc
The first supernova visible to the naked eye in 400 years

Core-collapse event

Post- and pre- explosion images from the AAT



SN 1987A – an example

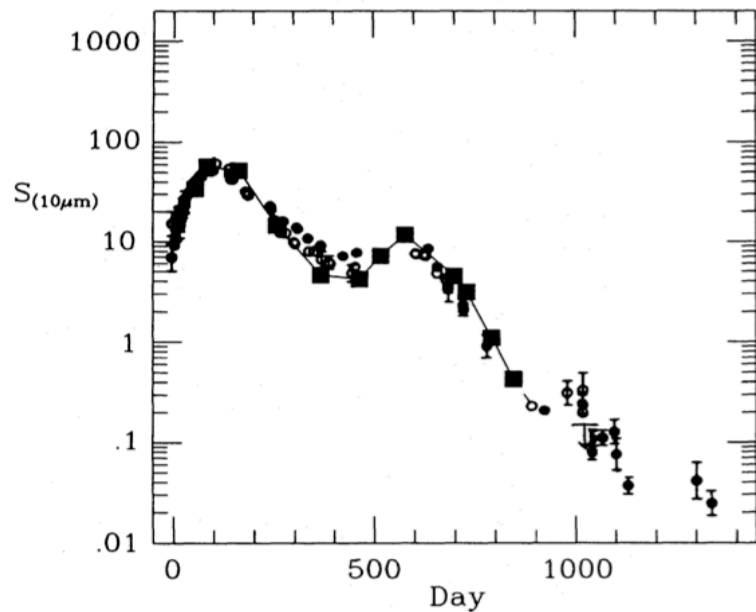


Figure 4. The 10- μ m continuum flux derived from the 8–13 μ m spectra (squares) compared with the photometric measurements made at CTIO (filled circles) and at ESO (open circles). Figure adapted from Suntzeff et al. (1991).

The mid-infrared spectrum

As the ejecta expanded, they cooled but the surface area increased and the flux increased at $10\mu\text{m}$, peaking after ~ 50 days.

With continued expansion, the density continued to decrease so that the material became optically thin after ~ 250 days, and the flux decreased. It became possible to measure the emission from the whole volume.

A number of rare IR fine-structure lines appeared allowing estimates of the mass of Co, Ni etc, initially as singly ionized species, but increasingly from neutral atoms after 1 year

The lines were broadened by the expansion speed of ~ 2000 km/s resulting in blends e.g. the line at $11.3\mu\text{m}$ is a blend of H 9-7, [Ni I] and [Cl I]

After a year, the mid-IR flux increased due to thermal emission from warm dust formed in the ejecta, preceded by emission from CO and SiO molecules

We can estimate the mass of emitting ions provided that the density is above the critical density so that the equations hold, and that the temperature of the ejecta is in the correct range to permit use of the Boltzmann approximation

524 P. F. Roche, D. K. Aitken and C. H. Smith

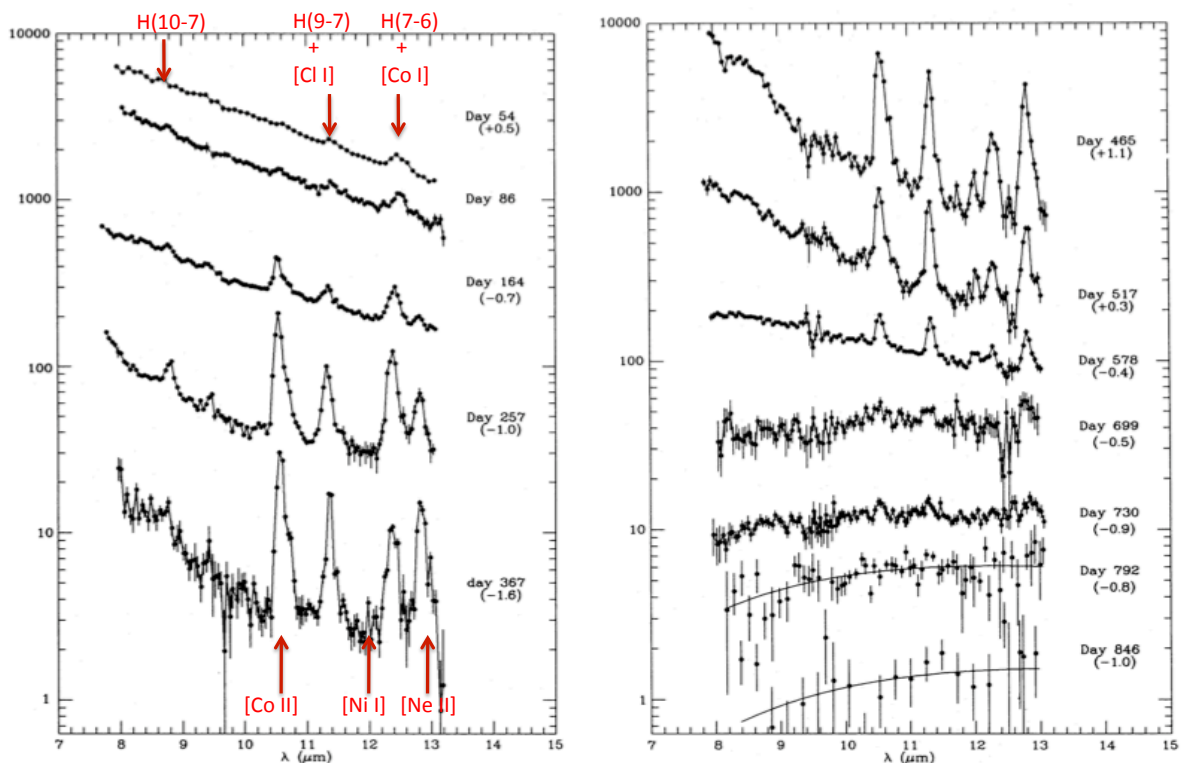


Figure 1. Spectra at 8–13 μm of SN 1987A. Error bars shown are 1 standard deviation of the mean and the flux is in units of $10^{-18} \text{ W cm}^{-2} \mu\text{m}^{-1}$. The logarithmic displacements of the spectra are given in brackets.

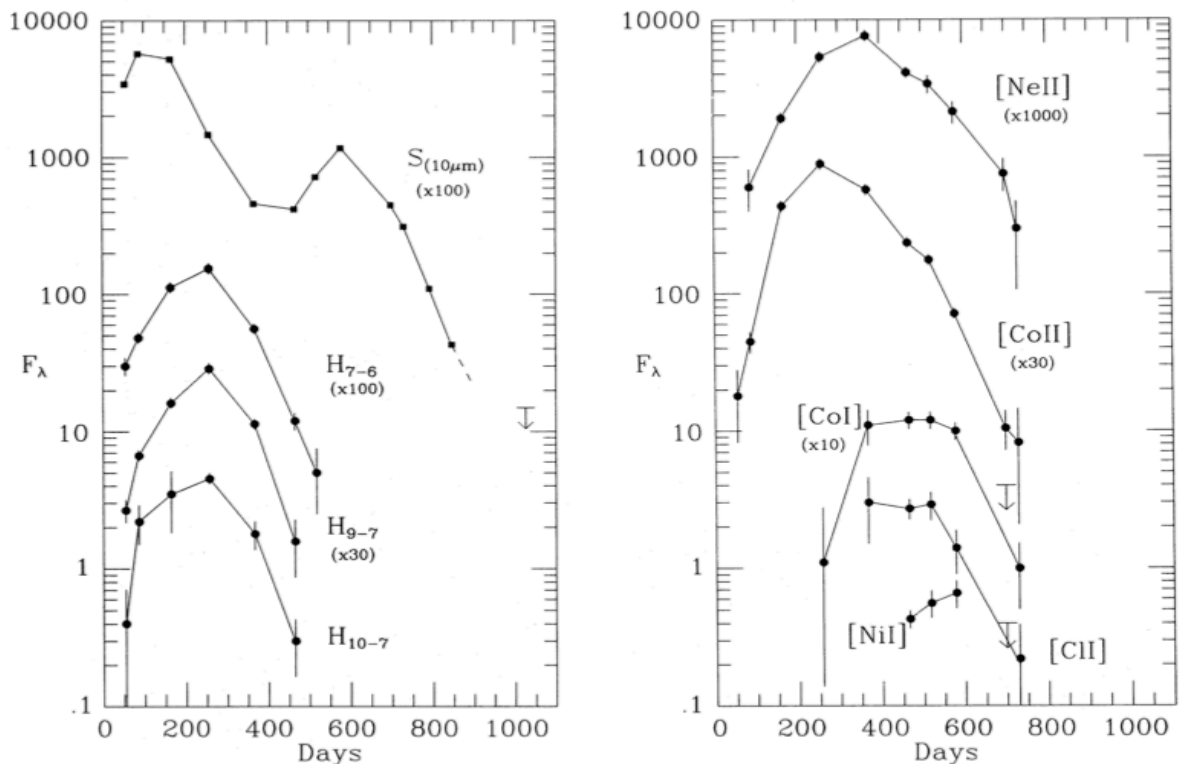


Figure 2. Evolution of the emission-line fluxes ($10^{-18} \text{ W cm}^{-2}$) and the 10-μm continuum (Jy). Upper limits shown are 3σ .

Mass estimates

We have (for $d=50\text{kpc}$) :

For $12.8\mu\text{m}$ NeII and $11.33\mu\text{m}$ Cl I :

$$A_{21} = 8.55 \text{ E-3, } 1.24 \text{ E-2,}$$

$$A_m = 20, \quad 35 \text{ AMU}$$

$$M_2 = 4\pi d^2 I_\lambda m_a \frac{\lambda_{21}}{hcA_{21}}$$

$$M_2 = 1.25 \times 10^5 I_\lambda A_m \frac{\lambda_{21}}{A_{21}}$$

Where I_λ is in Wm^{-2} , λ is in μm and A_m is the atomic number and the mass M is in solar masses
 On day 465, $I_{12.8\mu\text{m}} = 4.1 \times 10^{-14} \text{ Wm}^{-2}$, and $I_{11.3\mu\text{m}} = 2.7 \times 10^{-14} \text{ Wm}^{-2}$

With $T=3000 \text{ K}$, the Boltzmann exponential is 0.67, and the ratio of statistical weights (lower : upper) = 2, so the estimated mass of Ne^+ is $5 \times 10^{-4} M_\odot$ and of neutral Chlorine is $3.6 \times 10^{-4} M_\odot$.

Comparison with models suggests that Chlorine is predominantly neutral while Neon has a low ionization fraction as expected from the ionization balance of other elements.

Measurements of Co and Ni trace the changing ionization state of the ejecta and the radioactive decay of Cobalt formed by the decay of ^{56}Ni synthesised in the explosion ($0.07 M_\odot$ of Ni was formed)

Advantages of IR lines

At long wavelengths, the IR lines are relatively immune to the effects of interstellar extinction (which falls steeply as a function of λ) and so they can probe regions that are invisible at optical wavelengths or where only the front, lightly obscured regions are detected. They sample the whole volume of a nebula except for the densest, most obscured objects.

They provide some diagnostics of species that usually have weak or non-existent transitions at other wavelengths (e.g. Ne II)

The ground state fine-structure lines are insensitive to the electron temperature, and can often be well approximated by Boltzmann populations

BUT measurements at these wavelengths from the ground are hampered by the large thermal background from the atmosphere and telescope and molecular absorption bands in Earth's atmosphere.

Space telescopes – Spitzer, AKARI, Herschel and JWST can access the whole IR spectrum, and not just the atmospheric windows

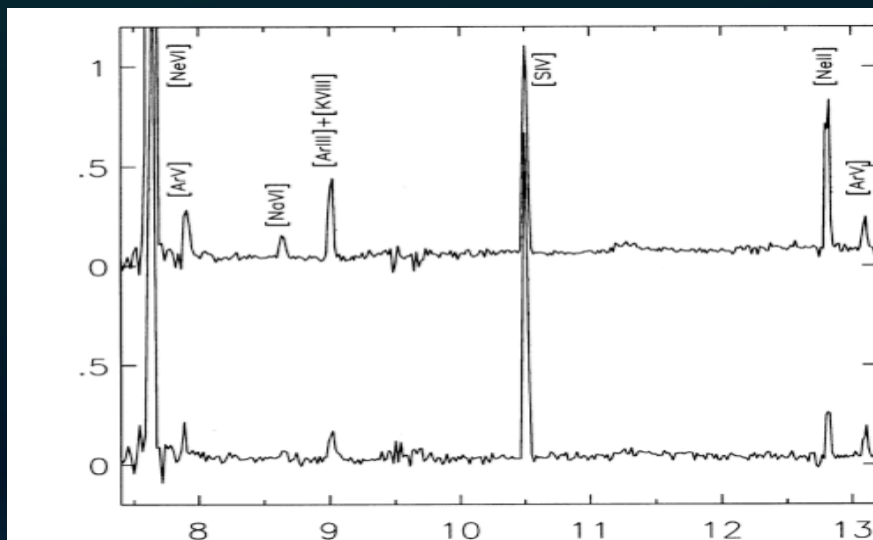


Figure 1. CGS3 spectra of NGC 6302 and NGC 6537. The spectrum with annotations is that of NGC 6302. Wavelengths are in microns, and flux densities are in $10^{-12} \text{ W m}^{-2} \mu\text{m}^{-1}$.

NGC 6302 is the Planetary nebula with the hottest known central star ($T^* \sim 250,000 \text{ K}$) and a high excitation spectrum, with emission lines from both Ne II and Ne VI (IP 21 & 126 eV). The lines of [A III], [S IV] and [Ne II] with IP in the range 20-40 eV are usually the strongest in typical photoionized nebulae.

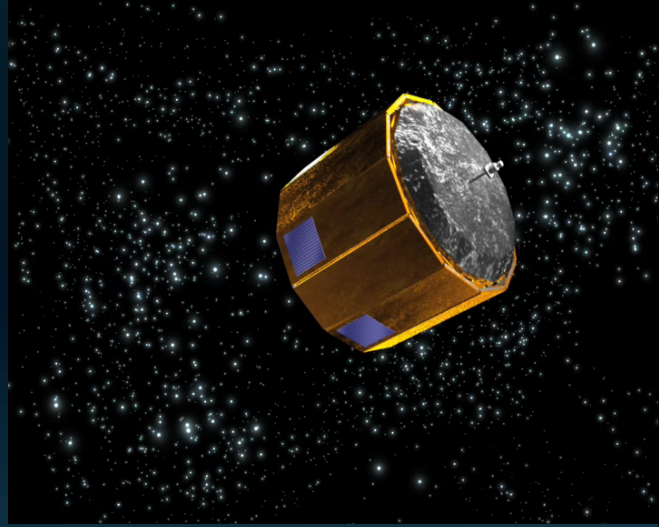


Astronomical Distances

While distances to nearby stars are well-measured through parallax, distance estimates to most objects are often very uncertain.

This will change radically over next few years when results from GAIA become available

GAIA will map precisely positions and velocities for ~1 Billion stars in the Milky Way



IR fine structure lines in nebulae

SN 1987A was a special case because the distance to the LMC is well known.

For most objects, this is not the case and so mass estimates are subject to large uncertainties.

However, we can obtain relative abundances by measuring the flux in a fine-structure line and comparing it to the flux in a hydrogen recombination line to measure $N_{\text{ion}}/N_{\text{H}}$. This works well if the extinction is well characterised and if the ionization fraction of hydrogen is known.

The bright H lines are at short wavelengths, and so infrared Bracket series lines are preferred to ensure that similar volumes are sampled.

e.g. for a dense nebula, measurements of a fine structure line and Br α ($n=5 \rightarrow 4$) would give:

$$\frac{F_{21}}{F_{\text{Br}\alpha}} = \frac{\frac{hc}{\lambda_{21}} N_2 A_{21}}{4\pi J_{\text{Br}\alpha} N_e N_p}$$

where $J_{\text{Br}\alpha}$ is the line emissivity, provided that the lines are emitted from the same volume. The fraction in the upper level can be estimated from the Boltzmann function for these IR ground state line. This can be rearranged to give N_2/N_p .

Radiative Recombination

To good accuracy, H is predominantly in the ground state in nebulae with $T \sim 10^4$ K.

Photoionization then requires photons with $E > 13.6$ eV. Electrons are ejected with $E' = E - 13.6$ and then quickly interact with other particles to give a \sim Maxwellian velocity distribution.

In turn these electrons will recombine via capture by protons into a bound state (generally not the ground state), releasing their energy $E_e + E_n$ and followed by a radiative cascade to the ground state.

The number of recombinations per unit volume per unit time is:

$$N_e N_p \sigma_{fb} f(v) v dv$$

Where $\sigma_{fb}(v)$ is the recombination cross section to a level. In practice, we are usually interested in the recombination coefficient summed over all bound states. Tables of total and individual recombination coefficients have been calculated, and give only slowly changing distributions as functions of N_e and T_e . By measuring a single H line, we can calculate the total recombination rate by applying appropriate factors.

Ionic abundances in the low density limit

In the low-density limit, use the Coronal approximation $N_2/N_1 = C_{12} N_e / A_{21}$

And expressing C_{12} in terms of the Collision strength Ω gives

$$\frac{N_2}{N_1} = \frac{8.63 \times 10^{-12} n_e \Omega}{A_{21} g_1 T_e^{1/2}} e^{-\Delta E/kT_e}$$

The density-normalised line luminosity is given by :

$$\frac{L_i}{n_e n_i} = \frac{hc}{\lambda_{21}} A_{21} \int \frac{N_2}{N_1 N_e} dV$$

Which can then be ratioed with the line luminosity from a nearby hydrogen line to estimate the ionic abundance, N_i/N_p if the fraction in the upper level can be estimated.

$$\frac{L_H}{n_e n_p} = \int \epsilon_v dV$$

Where $\epsilon_v = 4\pi j_v$ is the emissivity of the hydrogen line.